

## The Transcription Factor ETV1 Induces Atrial Remodeling and Arrhythmia

Carolin Rommel, Stephan Rösner, Achim Lothar, Margareta Barg, Martin Schwaderer, Ralf Gilsbach, Timo Bömicke, Tilman Schnick, Sandra Mayer, Sophia Doll, Michael Hesse, Oliver Kretz, Brigitte Stiller, Franz-Josef Neumann, Matthias Mann, Markus Krane, Bernd K. Fleischmann, Ursula Ravens, Lutz Hein

**Rationale:** Structural and electrophysiological remodeling of the atria are recognized consequences of sustained atrial arrhythmias, such as atrial fibrillation. The identification of underlying key molecules and signaling pathways has been challenging because of the changing cell type composition during structural remodeling of the atria.

**Objective:** Thus, the aims of our study were (1) to search for transcription factors and downstream target genes, which are involved in atrial structural remodeling, (2) to characterize the significance of the transcription factor ETV1 (E twenty-six variant 1) in atrial remodeling and arrhythmia, and (3) to identify ETV1-dependent gene regulatory networks in atrial cardiac myocytes.

**Methods and Results:** The transcription factor ETV1 was significantly upregulated in atrial tissue from patients with permanent atrial fibrillation. Mice with cardiac myocyte-specific overexpression of ETV1 under control of the myosin heavy chain promoter developed atrial dilatation, fibrosis, thrombosis, and arrhythmia. Cardiac myocyte-specific ablation of ETV1 in mice did not alter cardiac structure and function at baseline. Treatment with Ang II (angiotensin II) for 2 weeks elicited atrial remodeling and fibrosis in control, but not in ETV1-deficient mice. To identify ETV1-regulated genes, cardiac myocytes were isolated and purified from mouse atrial tissue. Active *cis*-regulatory elements in mouse atrial cardiac myocytes were identified by chromatin accessibility (assay for transposase-accessible chromatin sequencing) and the active chromatin modification H3K27ac (chromatin immunoprecipitation sequencing). One hundred seventy-eight genes regulated by Ang II in an ETV1-dependent manner were associated with active *cis*-regulatory elements containing ETV1-binding sites. Various genes involved in Ca<sup>2+</sup> handling or gap junction formation (*Ryr2*, *Jph2*, *Gja5*), potassium channels (*Kcnh2*, *Kcnk3*), and genes implicated in atrial fibrillation (*Tbx5*) were part of this ETV1-driven gene regulatory network. The atrial ETV1-dependent transcriptome in mice showed a significant overlap with the human atrial proteome of patients with permanent atrial fibrillation.

**Conclusions:** This study identifies ETV1 as an important component in the pathophysiology of atrial remodeling associated with atrial arrhythmias. (*Circ Res.* 2018;123:550-563. DOI: 10.1161/CIRCRESAHA.118.313036.)

**Key Words:** angiotensin II ■ atrial fibrillation ■ fibrosis ■ transcription factor ■ transcriptome

Multiple factors contribute to the development and progression of atrial fibrillation (AF).<sup>1</sup> Structural and electrophysiological remodeling of the atria are recognized consequences of sustained atrial arrhythmias, such as AF.<sup>2</sup> Atrial structural remodeling is characterized by fibrosis, atrial dilatation, and cardiac myocyte hypertrophy resulting in electrical disturbances and perpetuation of AF.<sup>1,2</sup>

Electrical and structural alterations result in stasis of blood and a prothrombotic state increasing the risk of ischemic stroke.<sup>1</sup>

**Editorial, see p 515**  
**In This Issue, see p 507**  
**Meet the First Author, see p 508**

In May 2018, the average time from submission to first decision for all original research papers submitted to *Circulation Research* was 13.37 days.

From the Institute of Experimental and Clinical Pharmacology and Toxicology, Faculty of Medicine (C.R., S.R., A.L., M.B., M.S., R.G., T.B., T.S., S.M., L.H.), Heart Center, Congenital Heart Defects and Pediatric Cardiology, Faculty of Medicine (T.S., B.S.), Medicine, Renal Division, Medical Center, Faculty of Medicine (O.K.), BIOS Centre for Biological Signaling Studies (L.H.), and Heart Center, Cardiology and Angiology I, Faculty of Medicine (A.L.), University of Freiburg, Germany; Heart Center, Cardiology and Angiology II, Freiburg-Bad Krozingen, Germany (T.B., F.-J.N.); Proteomics and Signal Transduction, Max Planck Institute of Biochemistry, Martinsried, Germany (S.D., M.M.); Institute of Physiology I, Life and Brain Center, Medical Faculty, University of Bonn, Germany (M.H., B.K.F.); III, Medicine, University Medical Center Hamburg-Eppendorf, Germany (O.K.); Cardiovascular Surgery, German Heart Center Munich at the Technische Universität München, Germany (M.K.); INSURE (Institute for Translational Cardiac Surgery), Cardiovascular Surgery, Munich, Germany (M.K.); DZHK (German Center for Cardiovascular Research), Partner Site Munich Heart Alliance, Munich, Germany (M.K.); Institute of Experimental Cardiovascular Medicine, University Heart Center Freiburg-Bad Krozingen, Germany (U.R.); and Pharmacology and Toxicology, Medical Faculty, Technische Universität Dresden, Germany (U.R.).

The online-only Data Supplement is available with this article at <https://www.ahajournals.org/doi/suppl/10.1161/CIRCRESAHA.118.313036>.

Correspondence to Lutz Hein, MD, Institute of Experimental and Clinical Pharmacology and Toxicology, Faculty of Medicine, University of Freiburg, Albertstrasse 25, 79104 Freiburg, Germany. Email [lutz.hein@pharmakol.uni-freiburg.de](mailto:lutz.hein@pharmakol.uni-freiburg.de)

© 2018 American Heart Association, Inc.

*Circulation Research* is available at <https://www.ahajournals.org/journal/res>

DOI: 10.1161/CIRCRESAHA.118.313036

## Novelty and Significance

### What Is Known?

- Structural and electrical remodeling are pathophysiological features of atrial arrhythmias, including atrial fibrillation.
- Angiotensin II facilitates atrial remodeling and fibrosis in experimental models, but intracellular signaling and transcription factors involved are only partially known.

### What New Information Does This Article Contribute?

- Expression level of the transcription factor ETV1 is increased in the atria from patients with permanent atrial fibrillation.
- In mice, overexpression of ETV1 in cardiac myocytes induces atrial remodeling, fibrosis, thrombosis, and arrhythmia, although ablation of ETV1 protects from angiotensin II–mediated atrial remodeling.
- Determination of RNA and open chromatin profiles by next-generation sequencing in atrial myocytes isolated from mouse and human hearts identified an ETV1-dependent gene network involved in atrial remodeling.

Atrial fibrillation is accompanied by changes in atrial wall structure, cell composition, and extracellular matrix deposition. Identification of molecular signaling pathways involved in this

atrial remodeling has been challenging because of the changing cellular composition of atria. We identified upregulation of the transcription factor ETV1 (E twenty-six variant 1) mRNA and protein in atrial tissue from patients with permanent atrial fibrillation. To determine functional significance of ETV1 in atrial cardiac myocytes, we generated mice with cell type–specific overexpression or ablation of ETV1. Overexpression of ETV1 in cardiac myocytes led to atrial enlargement, atrial fibrosis, thrombosis, and arrhythmia. In contrast, ETV1 knockout prevented atrial remodeling induced by chronic infusion of angiotensin II. To identify target genes that are regulated by angiotensin II in an ETV1-dependent manner, we isolated cardiac myocytes or their nuclei from mouse atria and RNA expression and open chromatin patterns were analyzed by next-generation sequencing. We identified >170 target genes of ETV1, including several genes involved in electrophysiological and hypertrophic remodeling of atrial myocytes. This network of ETV1-dependent genes in mouse atria was similar to the proteome signature of human atria in permanent atrial fibrillation. The findings provide insights into the molecular mechanisms involved in the pathogenesis of atrial fibrillation.

### Nonstandard Abbreviations and Acronyms

<b>α-MHC</b>	α-myosin heavy chain gene
<b>AF</b>	atrial fibrillation
<b>Ang II</b>	angiotensin II
<b>AT1R</b>	angiotensin receptors type 1
<b>AT2R</b>	angiotensin receptors type 2
<b>ATAC-seq</b>	assay for transposase-accessible chromatin sequencing
<b>ERK</b>	extracellular signal-regulated kinase
<b>ETV1</b>	E twenty-six variant 1
<b>FPKM</b>	fragments per kilobase of exon per million mapped reads
<b>GPCR</b>	G-protein–coupled receptors
<b>LV</b>	left ventricle
<b>MAPK</b>	mitogen-activated protein kinases
<b>MEF2</b>	myocyte enhancer factor 2
<b>MSK1</b>	mitogen- and stress-activated protein kinase 1
<b>RSK1</b>	ribosomal S6 kinase 1
<b>TGF-β1</b>	transforming growth factor-β1
<b>WT</b>	wild type

Ang II (angiotensin II) and other signaling molecules, including TGF-β1 (transforming growth factor-β1), play an important role in atrial and ventricular remodeling of the heart.<sup>3,4</sup> Increased Ang II levels and activation of intracellular signaling can be detected even before the development of atrial fibrosis.<sup>2</sup> Ang II, the active mediator of the renin-angiotensin system, results from cleavage of Ang I by the angiotensin-converting enzyme and elicits its downstream effects via binding to the AT<sub>1</sub>R and AT<sub>2</sub>R (angiotensin receptors type 1 and 2).<sup>5</sup> AT<sub>1</sub>R activation induces vasoconstriction, sodium and water retention, aldosterone and vasopressin release, stimulation of sympathetic tone, inflammation, fibrosis, and hypertrophy.<sup>6</sup> Interestingly, mice with cardiac myocyte-specific overexpression of angiotensin-converting enzyme or AT<sub>1</sub> receptors

develop severe atrial dilatation and AF without overt changes in ventricular structure.<sup>7,8</sup>

Many intracellular signaling pathways that coordinate the cardiac hypertrophic response are known.<sup>9</sup> Ang II and catecholamines bind to GPCR (G-protein–coupled receptors) leading to the activation of different intracellular signaling pathways including MAPK (mitogen-activated protein kinases), intracellular Ca<sup>2+</sup> release with activation of Ca<sup>2+</sup>-dependent cascades (eg, Ca<sup>2+</sup>/calmodulin-dependent protein kinase and calcineurin), or activation of protein kinase A.<sup>9</sup> Ultimately, overactivity of these intracellular signaling pathways leads to activation or repression of cardiac myocyte transcription.<sup>10,11</sup> Several transcription factors, including GATA (GATA-binding protein), MEF2 (myocyte enhancer factor 2), and the homeobox transcription factor NKX2.5 (NK2 homeobox 5) have been implicated in cardiac remodeling.<sup>11,12</sup> However, less is known about transcription factors which are involved in atrial remodeling in chronic heart disease.<sup>13</sup>

Thus, we searched for differential expression of transcription factors in human and mouse cardiac remodeling and identified ETV1 (E twenty-six variant 1) to be upregulated in cardiac atria from patients with AF. Our results demonstrate that cardiac myocyte-specific overexpression of ETV1 in the mouse induces atrial arrhythmia, atrial structural, and molecular remodeling. In contrast, cardiac myocyte-specific ablation of ETV1 leads to a protection against Ang II–mediated atrial remodeling. Furthermore, we identified active *cis*-regulatory regions in atrial cardiac myocytes and an ETV1-dependent gene regulatory network involved in atrial remodeling and arrhythmogenesis.

## Methods

### Data Availability

The authors declare that all supporting data are available within the article and its [Online Data Supplement](#).

All sequencing data sets reported in this article are deposited in the Short Read Archive at the National Center for Biotechnology Information (NCBI) under the BioProject ID PRJNA470521 for

human samples and PRJNA470522 for mouse data. Materials and further information are available upon personal request at the Institute of Experimental and Clinical Pharmacology and Toxicology, University of Freiburg, Germany.

### Human Cardiac Biopsies

Investigations of cardiac biopsies were approved by the ethics committees of the University of Freiburg (Germany) and the Medical Faculty of the Technical University Dresden (ethical approval No. 15.1/01031/006/2008 and No. EK790799) and conform with the principles outlined in the Declaration of Helsinki.

### Animal Procedures

All animal procedures were approved by the responsible Committee on the Ethics of Animal Experiments (Regierungspräsidium, Freiburg, Germany, permit numbers: G12/30 and G16/62), and they conformed to the Guide for the Care and Use of Laboratory Animals (2011).

### Generation of Mouse Models

Transgenic mice overexpressing *Etv1* under control of the cardiac myocyte-specific  $\alpha$ -myosin heavy chain gene promoter were generated by pronuclear injection (*Etv1* <sup>$\alpha$ MHC</sup>). For the generation of cardiac myocyte-specific ETV1-deficient mice (*Etv1*<sup>MLC2aCre</sup>), mice carrying a floxed *Etv1* allele<sup>14</sup> were crossed with MLC2a-Cre (Cre recombinase expression under control of the myosin light chain [*Myh7*] promoter) mice.<sup>15</sup>

### Ang II Stimulation In Vivo

Micro-osmotic pumps were used for continuous subcutaneously delivery of 2 mg kg<sup>-1</sup> d<sup>-1</sup> Ang II for 14 days.

### Electrocardiography

Electrocardiography was assessed in mice 1 week after birth during isoflurane anesthesia (2% Vol/Vol in O<sub>2</sub>). In adult mice, telemetry transmitters were implanted subcutaneously under isoflurane anesthesia (2% Vol/Vol in O<sub>2</sub>).

### Catheter Measurements

Mice were anesthetized and after dissection of the right carotid artery a 1.4F pressure catheter was introduced into the left ventricle (LV).

### Histological Analysis

For histological analysis, hearts were excised, fixed in paraformaldehyde solution, subsequently dehydrated, and embedded in paraffin and stained as described.<sup>16</sup> To evaluate cardiac myocyte size, LV sections were stained with wheat germ agglutinin-Alexa Fluor 488 conjugate.

### Isolation of Atrial Cardiac Myocyte Nuclei

Cardiac myocyte nuclei were isolated, stained with antibodies against phospholamban, and purified by fluorescence-assisted cell sorting as described previously.<sup>17</sup>

### Isolation of Atrial and Ventricular Cardiac Myocytes

Atrial and ventricular myocytes were enzymatically isolated by Langendorff perfusion followed by enzymatic digestion. Isolated atrial cardiac myocytes were picked individually under a microscope and processed for isolation of RNA.

### Gene Expression Analysis

Total RNA from atria and ventricles was isolated with the RNeasy Mini Fibrous Tissue Kit. Five hundred nanograms of RNA was transcribed, and RT-qPCR (quantitative reverse transcription PCR) was performed. For RNA sequencing, libraries were generated and sequencing was performed on a HiSeq 2500 (50 bp; Illumina).

### Assay for Transposase-Accessible Chromatin Sequencing

Isolated atrial cardiac myocyte nuclei were mixed with the transposition reaction mix (Nextera DNA Library Preparation Kit; Illumina) as described previously.<sup>18</sup>

### Chromatin Immunoprecipitation Sequencing

Chromatin was isolated from atrial cardiac myocytes (HL-1 cells [cardiac muscle cell line]<sup>19</sup>), sheared by sonication, and isolated following the manufacturer's manual of the ChIP-IT High Sensitivity Kit (Active Motif). Two micrograms of chromatin and 4  $\mu$ g of the antibody against H3K27ac (ab4729; Abcam) were used.

### General Bioinformatic Analysis

Computational analysis of sequencing data was performed with tools integrated in the Galaxy platform.<sup>20</sup> Sequencing reads were mapped with bowtie2<sup>21</sup> (chromatin immunoprecipitation sequencing [ChIP-seq], ATAC-seq [assay for transposase-accessible chromatin sequencing]) and RNA STAR (spliced transcripts alignment to a reference<sup>22</sup>; RNA-seq). Cuffdiff<sup>23</sup> was used to assess differential gene expression. DeepTools<sup>24</sup> were used for quality control, normalization, and genome-wide visualization. Peak identification was performed with MACS2 (model-based Analysis of ChIP-Seq 2;  $q < 0.05$ ).<sup>25</sup>

### Human AF Proteome

Mass spectrometry-based proteome data from patients with permanent AF were reanalyzed for this study.<sup>26</sup> Details about sample preparation for mass spectrometry (MS) analysis, liquid chromatography-MS analysis, and MS data analysis are described in Doll et al.<sup>26</sup>

### Statistics

Data were displayed as mean  $\pm$  SEM. Student *t* test, 1-way, or 2-way ANOVA followed by Bonferroni post hoc test were used for statistical analysis of normally distributed data sets. Nonparametric Mann-Whitney test or Kruskal-Wallis ANOVA followed by Dunn post hoc test was performed for data sets without evidence for normal distribution. *P* values  $< 0.05$  were considered statistically significant.

## Results

### ETV1 Is Upregulated in Human and Mouse Heart Disease

During the search for genes differentially regulated in human heart disease, we found upregulation of the transcription factor ETV1 mRNA and protein in cardiac atria from patients with permanent AF (Figure 1A and 1B). As *Etv1* expression levels were 5-fold higher in atria than in ventricles (Figure 1C), we sought to further characterize the functional significance of ETV1 in atria. Expression of *Etv1* mRNA was higher in the free atrial wall when compared with the sinus node<sup>27</sup> (Figure 1D), but it did not differ between left and right atria (Figure 1E).

### Cardiac Myocyte-Specific Overexpression of ETV1 Increases Mortality Rate

To investigate the cardiac function of ETV1, we generated 2 genetically modified mouse models. First, transgenic mice overexpressing *Etv1* under control of the cardiac myocyte-specific  $\alpha$ -MHC ( $\alpha$ -myosin heavy chain gene) promoter (*Etv1* <sup>$\alpha$ MHC</sup>) were generated by pronuclear injection (Figure 1F), and 2 independent transgenic lines were established which showed similar phenotypes. *Etv1* overexpression led to increased atrial and ventricular *Etv1* mRNA and ETV1 protein levels in transgenic mice (Figure 1G and 1H; Online Figure IA and IB). Surprisingly, *Etv1* <sup>$\alpha$ MHC</sup> mice showed a significantly increased mortality rate compared with wild-type (WT) littermates (Figure 1I). *Etv1* <sup>$\alpha$ MHC</sup> transgenic mice showed normal LV function and morphology when compared with WT littermates 12 weeks after birth (Online Figure IIA through IIG).

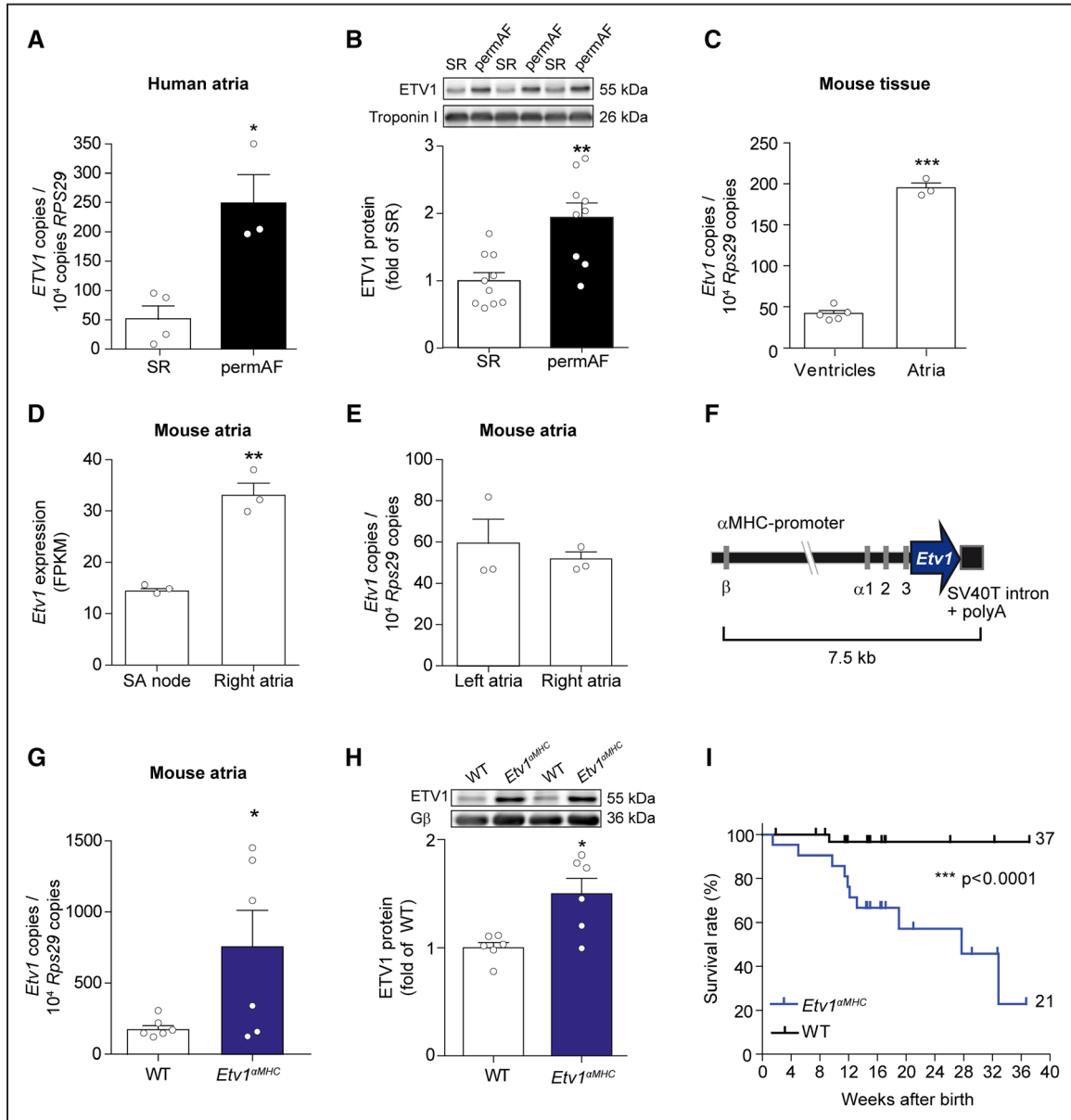


**Figure 1.** Increased expression of the transcription factor ETV1 (E twenty-six variant 1) in atria from patients with permanent atrial fibrillation and in transgenic mice under control of the  $\alpha$ -MHC ( $\alpha$ -myosin heavy chain gene) promoter. **A**, ETV1 mRNA levels in human right atrial appendages from patients with permanent atrial fibrillation (perMAF) compared with patients in sinus rhythm (SR) as determined by RT-qPCR (n=3–4). **B**, Western blot analysis of ETV1 protein expression in right atrial appendages from patients with perMAF and SR (n=9–10). **C**, *Etv1* mRNA levels in adult mouse atria compared with ventricle as determined by RT-qPCR (n=3–5). **D**, *Etv1* mRNA expression in right atrium compared with the sinoatrial (SA) node. RNA-seq data were reanalyzed<sup>27</sup> (n=3, Cuffdiff). **E**, Expression levels of *Etv1* were measured by RT-qPCR in left and right atria from adult wild-type (WT) mice (n=3 per group, Student *t* test). **F**, Schematic diagram of the *Etv1* transgenic vector under control of the cardiac-specific  $\alpha$ -MHC promoter ( $\beta$ ,  $\alpha$ 1–3: exons of  $\beta$ - and  $\alpha$ -MHC genes; SV40T: Simian virus 40 T antigen). **G**, Atrial *Etv1* gene expression in WT and transgenic *Etv1* <sup>$\alpha$ MHC</sup> mice (n=6 per genotype, Student *t* test). **H**, Western blot analysis of ETV1 protein expression in WT and *Etv1* <sup>$\alpha$ MHC</sup> atria (n=6, Student *t* test). **I**, Kaplan-Meier survival curve of WT (black) and *Etv1* <sup>$\alpha$ MHC</sup> transgenic mice (blue). *Etv1* <sup>$\alpha$ MHC</sup> transgenic mice showed a significantly reduced survival compared with WT animals (WT n=37, *Etv1* <sup>$\alpha$ MHC</sup> n=21). Mean $\pm$ SEM; \**P*<0.05, \*\**P*<0.01, \*\*\**P*<0.001.

### Overexpression of *Etv1* Leads to Arrhythmia in Adult *Etv1* <sup>$\alpha$ MHC</sup> Mice

To further search for causes of premature death of *Etv1* <sup>$\alpha$ MHC</sup> mice, ECG was performed in mice 1 week after birth. At this time point, ECG analysis showed no differences between genotypes (Figure 2A). Heart rate, QRS interval, P-wave duration, and PR interval were not altered in young *Etv1* <sup>$\alpha$ MHC</sup> animals (Figure 2B through 2E). Next, ECG telemetry devices were implanted in adult mice (12 weeks; Figure 2F through 2J; Online Figures IIIA and IV). At this age, *Etv1* <sup>$\alpha$ MHC</sup> mice

showed bradycardia and a loss of P waves (Figure 2F and 2G). Female (Figure 2F through 2J) and male (Online Figure IIIA and IIIB) *Etv1* <sup>$\alpha$ MHC</sup> mice showed the same phenotype. Compared with young mice, adult *Etv1* <sup>$\alpha$ MHC</sup> animals showed arrhythmias at 12 weeks of age (Figure 2K and 2L, Online Figures IIIB and IV). For analysis of arrhythmias, successive RR intervals were plotted against the immediately preceding RR intervals. WT mice showed a typical torpedo pattern associated with normal SR (Figure 2M), whereas adult *Etv1* <sup>$\alpha$ MHC</sup> mice displayed an island type A pattern which is typical for

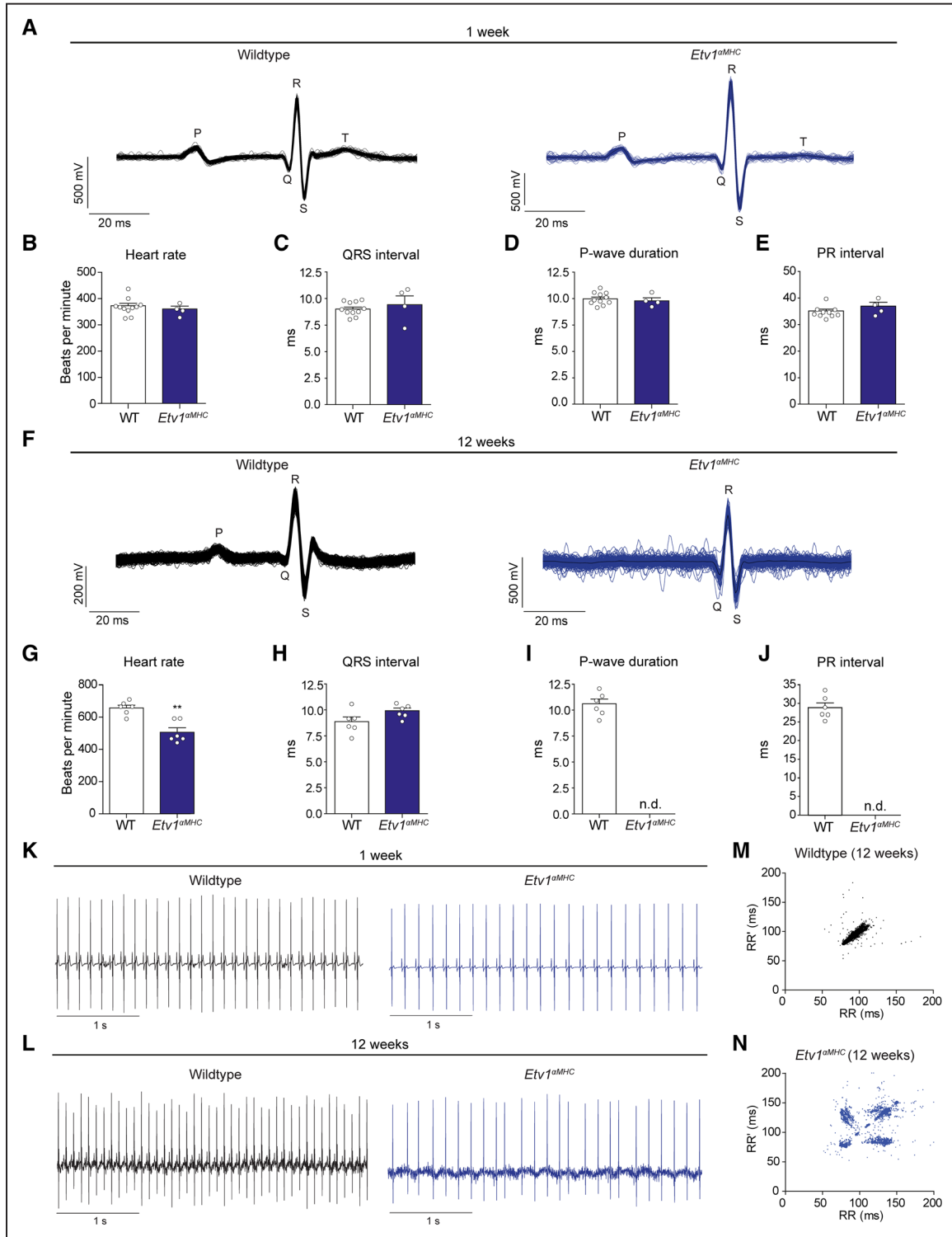


**Figure 2. Overexpression of the transcription factor ETV1 (E twenty-six variant 1) leads to arrhythmia in adult *Etv1<sup>αMHC</sup>* mice.** **A**, Representative ECG recordings of wild-type (WT) (black) and *Etv1<sup>αMHC</sup>* transgenic mice (blue) 1 week after birth. **B–E**, Quantification of **(B)** heart rate, **(C)** QRS interval, **(D)** P-wave duration, and **(E)** PR interval (n=4–11). **F**, Representative ECG recordings of adult WT (black) and *Etv1<sup>αMHC</sup>* transgenic mice (blue) 12 weeks after birth. **G–J**, Quantification of **(G)** heart rate, **(H)** QRS interval, **(I)** P-wave duration, and **(J)** PR interval (n=6 per genotype; n.d., not detectable). **K–N**, Heart rhythm. **K**, Representative ECG recordings of WT (black) and *Etv1<sup>αMHC</sup>* transgenic mice (blue) 1 week after birth. **L**, Representative ECG recordings of adult WT and *Etv1<sup>αMHC</sup>* transgenic mice (12 weeks). There were no differences between the genotypes 1 week after birth. Adult *Etv1<sup>αMHC</sup>* transgenic mice showed arrhythmia. **M**, **N**, Lorenz (Poincaré) plot for analysis of heart rate variability. The duration of an RR interval (x axis) is plotted against the duration of the following RR interval (RR'; y axis). **M**, WT mice (black) showed a typical torped pattern associated with normal sinus rhythm.<sup>28</sup> **N**, *Etv1<sup>αMHC</sup>* transgenic mice (blue) showed an island type A pattern associated with atrial arrhythmia.<sup>28</sup> Mean±SEM; \*\*P<0.01.

atrial arrhythmia (Figure 2N).<sup>28</sup> Analysis of individual ECGs of 12-week-old mice showed loss of P waves in all transgenic mice (Figure 2F) with different ECG patterns in individual *Etv1<sup>αMHC</sup>* animals (Online Figure IVG through IVL). Although some mice showed regularly spaced RR intervals (Online Figure IVG and IVI), others had irregular RR intervals (Online Figure IVK) or varying morphology of QRS complexes (Online Figure IVH, IVJ, and IVL).

### Etv1<sup>αMHC</sup> Mice Display Severe Atrial Remodeling

To determine whether atrial arrhythmia in *Etv1<sup>αMHC</sup>* mice was accompanied by structural changes, hearts were analyzed using morphological and histological approaches. Cardiac sections stained with hematoxylin and eosin from mice 1 week after birth showed no morphological differences between genotypes (Figure 3A). In contrast, adult *Etv1<sup>αMHC</sup>* mice displayed enlargement and dilatation of left and right atria (Figure 3B). Moreover, *Etv1<sup>αMHC</sup>* mice had an increased weight of left and right atria compared with WT animals (Figure 3C; Online Figure IIIC), and 4 out of 6 *Etv1<sup>αMHC</sup>* mice developed atrial thrombi by age of 12 weeks (Figure 3D). Interstitial fibrosis, identified by Sirius red staining, was strongly induced in *Etv1<sup>αMHC</sup>* atria (Figure 3E). Expression of vimentin (*Vim*) and the myofibroblast marker gene  $\alpha$ -smooth muscle actin (*Acta2*) was increased in *Etv1<sup>αMHC</sup>* atria (Figure 3F). In addition, Western blot analysis of caldesmon, a major Ca<sup>2+</sup>-binding protein in the sarcoplasmic reticulum, was decreased in atria from *Etv1<sup>αMHC</sup>* mice (Figure 3G). Electron microscopy revealed significant structural remodeling of *Etv1<sup>αMHC</sup>* atria 12 weeks after birth, whereas WT atria showed a normal dense and organized sarcomere structure (Figure 3H and 3I; Online Figure V). *Etv1<sup>αMHC</sup>* atria were characterized by abundant fibroblasts, interstitial collagen fibers, and loss of cardiac myocyte interfibrillar mitochondria and sarcomere structure (Figure 3H and 3I; Online Figure V).

Both *Etv1<sup>αMHC</sup>* transgenic lines showed a similar phenotype with atrial remodeling and arrhythmia. Transgenic mice from line number 2 were characterized by a higher transgene copy number (Online Figure VIA) which was also accompanied by premature death. At the age of 17 to 33 weeks, *Etv1<sup>αMHC</sup>* animals displayed massive atrial enlargement and thrombi (Online Figure VIF). In these moribund mice, there were also reductions of LV contractility and relaxation (Online Figure VIC through VIE), likely because of obstruction of ventricular inflow and ineffective atrial emptying because of atrial arrhythmia.

### Cardiac Myocyte-Specific Ablation of ETV1 Expression

To further determine the functional significance of ETV1 in the heart, mice with specific ablation of *Etv1* in cardiac myocytes (*Etv1<sup>MLCCre</sup>*) were generated by breeding mice carrying a floxed *Etv1* allele<sup>14</sup> with MLC2a-Cre mice<sup>15</sup> (Figure 4A). Exon 11 which encodes the ETS-binding domain was removed using the Cre/loxP system. *Etv1* mRNA was significantly reduced in cardiac myocytes from *Etv1<sup>MLCCre</sup>* mice, whereas *Etv1* expression was not changed in nonmyocytes (Figure 4B). *Etv1<sup>MLCCre</sup>* mice were viable and showed normal survival rates (Online Figure VIIA).

Ang II is known to play an important role in atrial remodeling and fibrillation<sup>29</sup>; mice were treated with Ang II for 14

days via osmotic pumps. ECG analysis revealed no irregularities in *Etv1<sup>MLCCre</sup>* and control mice at baseline or after Ang II stimulation (Online Figure VIIIA through VIIII). Heart rate, QRS interval, P-wave duration, and PR interval (Online Figure VIIIC through VIIIF) were not different in *Etv1<sup>MLCCre</sup>* animals compared with control animals. Both genotypes showed regular SR at baseline and after Ang II stimulation (Online Figure VIIIG and VIIIH). In addition, Lorenz (Poincaré) plots from control and *Etv1<sup>MLCCre</sup>* animals displayed a torpedo pattern associated with SR (Online Figure VIIII and VIIIJ).<sup>28</sup>

LV contractile function, heart rate, and LV wall dimensions at baseline and after Ang II treatment did not differ between *Etv1<sup>MLCCre</sup>* and control mice (Online Figure IXA through IXF). LV morphology was similar between genotypes at baseline and after Ang II stimulation (Online Figure XA through XH). Ang II stimulation led to an increased connective tissue growth factor (*Ctgf*) expression in control and *Etv1<sup>MLCCre</sup>* ventricles (Online Figure XJ).

### Etv1 Knockout Mice Are Protected From Atrial Remodeling After Ang II Stimulation

Four-chamber sections stained with hematoxylin and eosin from adult *Etv1<sup>MLCCre</sup>*, and control mice showed no morphological differences between the genotypes (Figure 4C). Although Ang II stimulation did not affect atrial weight in both genotypes (Figure 4D), it caused severe atrial fibrosis in control but not in *Etv1<sup>MLCCre</sup>* mice (Figure 4E through 4G). Ang II stimulation induced mRNA expression of *Vim* in atria from control animals, although this upregulation was prevented in *Etv1<sup>MLCCre</sup>* mice (Figure 4H). Electron microscopy revealed no structural changes in the atria from both genotypes at baseline (Figure 4I). Atrial mRNA expression of the myocyte-specific myosin heavy polypeptide 6 (*Myh6*) gene did not differ between genotypes at baseline. *Myh6* expression was significantly reduced in control atria after Ang II stimulation, whereas this downregulation was significantly attenuated in *Etv1<sup>MLCCre</sup>* atria (Figure 4J).

### ETV1-Dependent Atrial Transcriptome

To determine the molecular basis of the protective effect of ETV1 ablation in atria, we performed RNA-seq in atria from control and *Etv1<sup>MLCCre</sup>* mice without or after Ang II stimulation (Figure 5A). Ang II stimulation induced gene expression changes of 2527 genes in control atria and 1293 genes in *Etv1<sup>MLCCre</sup>* atria (Online Figure XI; Online Table III). Eight hundred thirty genes were induced and 510 genes showed decreased expression after Ang II stimulation in control atria, although these genes were not significantly regulated in *Etv1<sup>MLCCre</sup>* atria (Figure 5A; Online Table IV). Gene ontology analysis of genes upregulated after Ang II stimulation in control atria and not regulated in *Etv1<sup>MLCCre</sup>* atria (Figure 5A, group 1) showed a significant enrichment for genes involved in cytoskeleton organization, cell-substrate adhesion, adherens junction, and proteinaceous extracellular matrix. Gene ontology analysis of the second group including genes downregulated after Ang II stimulation in control atria and no regulation in *Etv1<sup>MLCCre</sup>* atria (group 2) showed enrichment for genes involved in mitochondrial and metabolic pathways (Figure 5A). Expression of genes involved in mitochondrial function, Ca<sup>2+</sup> handling, and ion channels was regulated by Ang II in control but not in ETV1-deficient atria (Figure 5B and 5C). These findings demonstrate

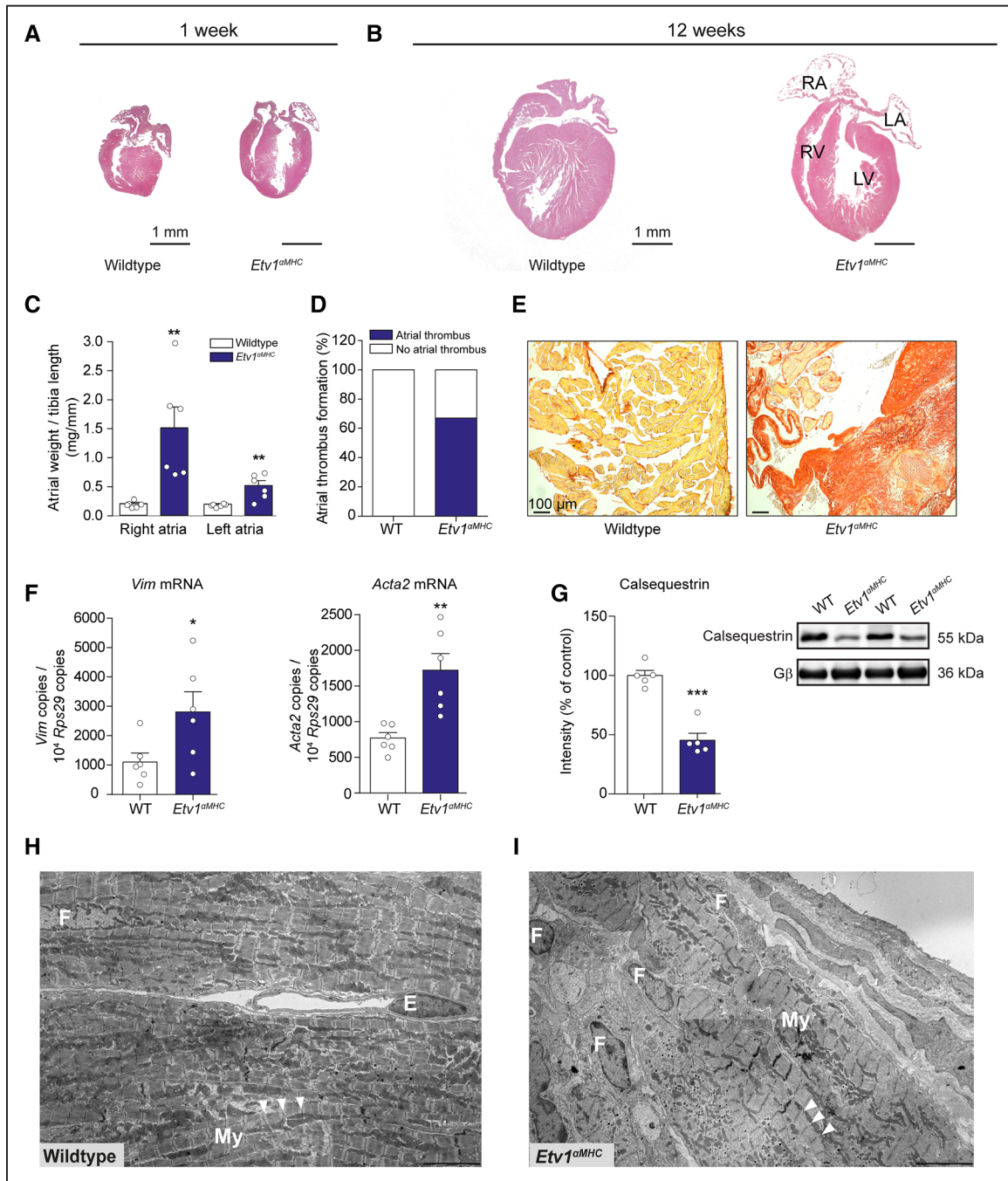


**Figure 3. Cardiac myocyte-specific overexpression of ETV1 (E twenty-six variant 1) leads to structural remodeling of the atria.** **A, B,** Cardiac sections of hematoxylin and eosin stained hearts from *Etv1<sup>αMHC</sup>* and wild-type (WT) animals at the age of **A,** 1 week after birth and **B,** 12 weeks, respectively (scale bar, 1 mm). **C,** Atrial weight/tibia length ratios (n=6 per genotype). **D,** *Etv1<sup>αMHC</sup>* mice show atrial thrombus formation compared with WT animals (n=6 per group, Fisher exact test, *P*=0.06). **E,** Atrial fibrosis identified by Sirius red staining in adult WT and *Etv1<sup>αMHC</sup>* atria (scale bar, 100 μm). **F,** Expression levels of vimentin (*Vim*), a marker for fibrosis, and the myofibroblast marker gene smooth muscle α-actin (*Acta2*) were measured by RT-qPCR in left atria from adult mice (n=6 per genotype). **G,** Western blot analysis of calsequestrin in right atria from adult mice (n=6 per genotype). **H, I,** Electron microscopy of left atria from adult *Etv1<sup>αMHC</sup>* and WT animals. Cardiac myocytes in WT atria showed a dense and organized sarcomere structure with Z-lines (arrowheads). Atria from *Etv1<sup>αMHC</sup>* animals showed increased abundance of fibroblasts. (scale bars, 5 μm). Mean±SEM; \**P*<0.05; \*\**P*<0.01; \*\*\**P*<0.001. E indicates endothelial cell; F, fibroblast; LA, left atrium; LV, left ventricle; My, myocyte; RA, right atrium; and RV, right ventricle.

that ablation of *Etv1* in cardiac myocytes protects atria from structural and molecular remodeling induced by Ang II.

### Comparison With Human AF

For comparison of our mouse model with human permanent AF, we analyzed the atrial proteome and cardiac myocyte nuclear transcriptome (Figure 5D). In atria from patients with

permanent AF,<sup>26</sup> 1237 proteins were differentially expressed when compared with control atria (Figure 5D). To determine, which of these proteins are expressed in atrial cardiac myocytes, we isolated cardiac myocyte nuclei and subjected these to RNA-seq, identifying 1099 genes which were expressed at 1 FPKM (fragments per kilobase per million mapped reads) or higher (Figure 5E). Differential protein expression in human

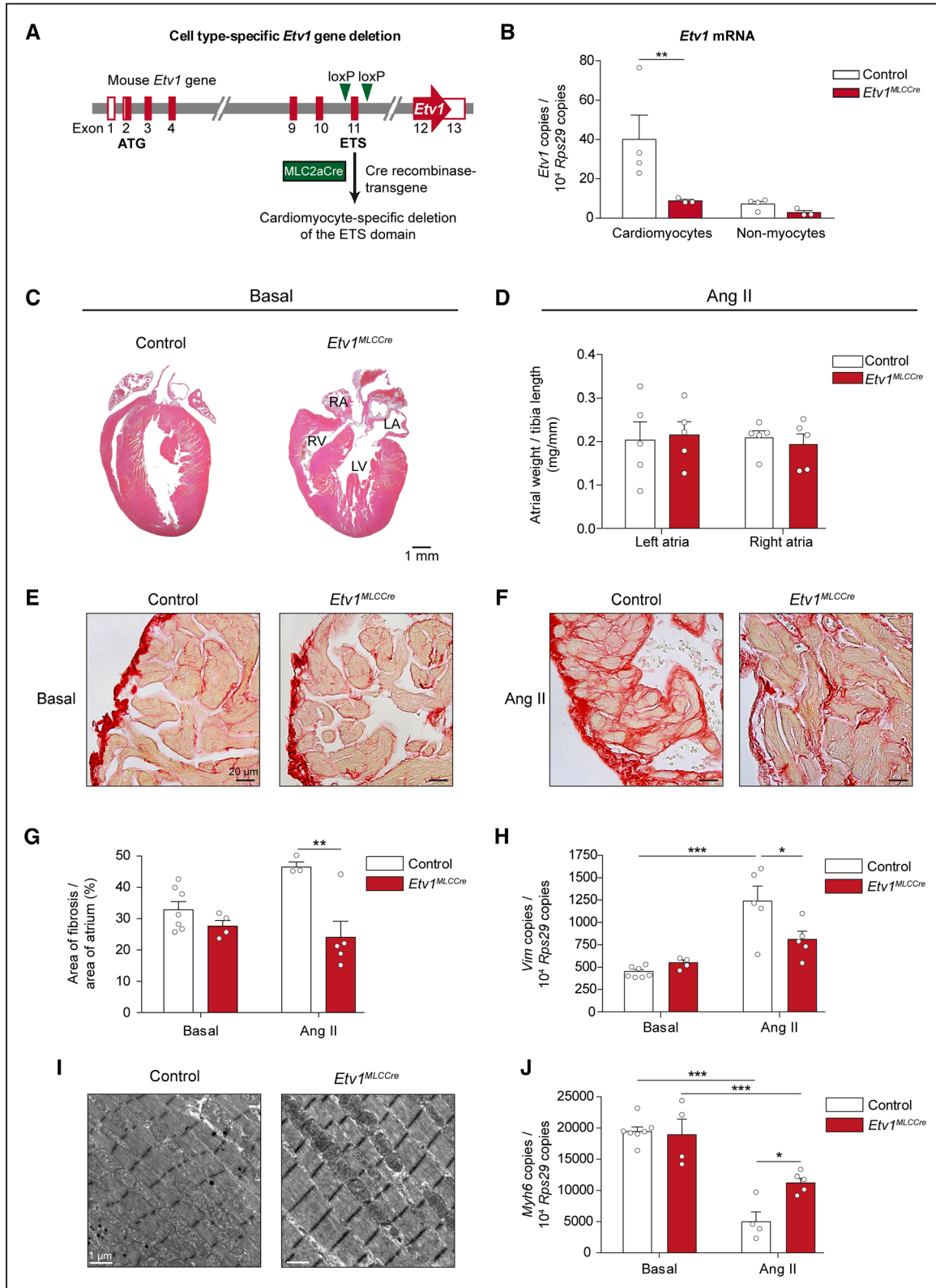


**Figure 4.** *Etv1*<sup>MLCCre</sup> mice are protected from structural remodeling after angiotensin II stimulation. **A**, Schematic diagram of the *Etv1* (*E* twenty-six variant 1) gene targeting construct with 2 loxP sites (green arrowheads) that flank exon 11, encoding the ETS DNA-binding domain of the Etv1 protein. Targeted deletion of the *Etv1* gene in cardiac myocytes is achieved by crossing the floxed *Etv1* allele with MLC2a-Cre recombinase-expressing mice. **B**, *Etv1* mRNA expression was significantly reduced by *Etv1* gene targeting in cardiac myocytes but not in nonmyocytes (n=3-4). **C**, Cardiac sections of hematoxylin and eosin stained hearts from adult *Etv1*<sup>MLCCre</sup> and control animals (scale bar, 1 mm). **D**, Atrial weight/tibia length ratios after 2 weeks of angiotensin II (Ang II) stimulation (n=4-7). **E, F**, Atrial fibrosis determined by Sirius red staining in control and *Etv1*<sup>MLCCre</sup> atria without treatment (**E**) and after 2 weeks of Ang II stimulation (**F**; scale bar, 20  $\mu$ m). **G**, Quantification of fibrosis (n=3-7). **H**, Expression levels of the fibroblast marker gene vimentin (*Vim*) in left atria at the basal state and after 2 weeks of Ang II stimulation. mRNA expression was measured by RT-qPCR. Ribosomal protein S29 (*Rps29*) was used as (Continued)

**Figure 4 Continued.** internal control (n=4–7 basal, n=5 per genotype Ang II). I, Electron microscopy of left atria from adult *Etv1<sup>MLCCre</sup>* and control animals (scale bar, 1  $\mu$ m). J, Expression levels of the myocyte-specific myosin heavy polypeptide 6 (*Myh6*) gene in left atria at the basal state and after 2 weeks of Ang II stimulation (n=4–7 basal, n=5 per genotype Ang II). Mean $\pm$ SEM; \* $P$ <0.05; \*\* $P$ <0.01; \*\*\* $P$ <0.001. LA indicates left atrium; LV, left ventricle; RA, right atrium; and RV, right ventricle.

AF identified 155 proteins which were also regulated at the RNA level in mouse atria by Ang II/ETV1 (Figure 5F; Online Table V). Taken together, these findings indicate that our mouse model of Ang II/ETV1-dependent atrial remodeling is highly congruent with human permanent AF.

### Chromatin Accessibility and Gene Expression in Mouse Atrial Cardiac Myocytes

To search for downstream genes specifically regulated by ETV1 in cardiac myocytes, we first established a method to isolate mouse atrial cardiac myocytes and nuclei for transcriptome analysis and for profiling of chromatin accessibility, respectively. Overall, 371 genes were differentially expressed in atrial versus ventricular cardiac myocytes (Online Figure XII). Two hundred two genes showed significantly higher expression levels in atrial versus ventricular myocytes, whereas 169 genes were preferentially expressed in ventricular myocytes (Online Figure XIIB). Genes that were enriched in atrial cardiac myocytes were involved in processes like muscle adaptation, ventricular cardiac muscle tissue development, and positive regulation of muscle contraction (Online Figure XIIC through XIIE).

To determine the regulatory landscape of atrial cardiac myocytes, fluorescence-activated sorting of cardiac nuclei was used (Figure 6A through 6C). Chromatin accessibility was analyzed by ATAC-seq (assay for transposase-accessible chromatin sequencing). Ranking of genes according to their gene expression level showed a correlation of gene expression and chromatin accessibility at promoter regions (Figure 6D). Genes with very low expression levels (<1 FPKM) displayed no chromatin accessibility at promoter regions (Figure 6D). In addition, we performed chromatin immunoprecipitation for the active histone modification H3K27ac followed by high-throughput sequencing (ChIP-seq) to identify putative active regulatory elements in atrial cardiac myocytes. Overall, 9340 regions with active signatures, including chromatin accessibility and enrichment of H3K27ac, were identified (Figure 6E and 6F). Two thousand thirty-five of these H3K27ac positive, ETV1 motif-containing accessible regions contained at least 1 ETV1-binding motif (Figure 6F), and they were predominantly found in promoter, intronic, and intergenic regions (Figure 6G). Further, we investigated whether ETV1-binding motifs were colocalized with binding motifs of transcription factors associated with AF like TBX5,<sup>30</sup> NKX2.5,<sup>31</sup> and GATA4<sup>32,33</sup> in ATAC peaks (Figure 6H). Colocalization with a least one additional transcription factor motif was found in 64.4% of ETV1-containing ATAC peaks (1310; Figure 6H). Interestingly, nearly half of these ATAC peaks (47.8%, 973) contained ETV1- and TBX5-binding sites.

### Identification of ETV1 Target Genes in Atrial Cardiac Myocytes

We next searched for genes which are regulated by Ang II and ETV1 (data set in Figure 5A) and are associated with H3K27ac positive, ETV1 motif-containing accessible regions in mouse atrial cardiac myocytes (data set in Figure 6F). We identified

178 genes which were significantly regulated by Ang II stimulation in control atria, but not in ETV1-deficient atria and were also associated with active accessible regions containing ETV1-binding sites (Figure 7A; Online Table VI). Several of these genes have previously been associated with atrial arrhythmia or cardiac remodeling. To further validate these findings, the expression pattern of 18 candidates out of these 178 genes (Figure 7A) which have previously been associated with atrial arrhythmia was tested in ETV1-deficient (Figure 7B) and in ETV1-transgenic atria (Online Figure XIII) by RNA-seq and by quantitative RT-PCR, respectively. Ten genes showed opposing patterns of regulation in knockout and in transgenic atria (Figure 7B; Online Figure XIII A through XIII J). Ablation of ETV1 prevented the Ang II-mediated downregulation of potassium channels (*Kcnh2*, *Kcnk3*), genes involved in Ca<sup>2+</sup> handling, and gap junction formation (*Ryr2*, *Atp2a2*, *Jph2*, *Gja5*) as well as the transcription factor *Tbx5* (Figure 7B; Online Figure XIII). Moreover, ETV1 ablation prevented the Ang II-mediated upregulation of several genes (eg, *Cib1*, *Bmp1*, *Ilk*, Figure 7B and Online Figure XIII). Representative traces display genomic regions containing *Cib1*, *Jph2*, and *Gja5* which show Ang II/ETV1-dependent gene expression changes and are associated with active accessible regions containing ETV1-binding sites in atrial cardiac myocytes (Figure 7C through 7E). Together, these results strongly support that ETV1 orchestrates the regulation of a transcriptional network that drives atrial remodeling.

### Discussion

In this study, we identified an essential role of the E twenty-six (ETS) transcription factor ETV1 in Ang II-induced atrial remodeling. ETV1 was significantly upregulated in atrial tissue from patients with permanent AF and was highly expressed in atria versus ventricles. Cardiac myocyte-specific overexpression of ETV1 in mice induced atrial remodeling and arrhythmia, thrombus formation, and increased mortality. In contrast, ablation of ETV1 expression in cardiac myocytes protected mice from Ang II-induced atrial structural and molecular remodeling. Numerous genes which have previously been associated with AF or cardiac remodeling were regulated by Ang II in an ETV1-dependent manner and were associated with active ETV1-containing *cis*-regulatory elements in atrial cardiac myocytes. The ETV1-dependent transcriptome in mouse atria showed significant overlap with the human atrial proteome of patients with permanent AF. These results suggest that ETV1 may be an important mediator of arrhythmia-associated atrial remodeling.

Recently, ETV1 was identified as an important factor for the development of the fast conduction system consisting of atrial cardiac myocytes and the ventricular His-Purkinje network.<sup>34</sup> The present mouse model of ETV1 ablation (*Etv1<sup>MLCCre</sup>*) shows similarities but also differences when compared with the model used by Shekhar et al.<sup>34</sup> Shekhar's group used a mouse model with constitutive deletion of exon 2 of the *Etv1* gene by insertion of a nuclear localized  $\beta$ -galactosidase, thus resulting in a hypomorphic *Etv1* allele in

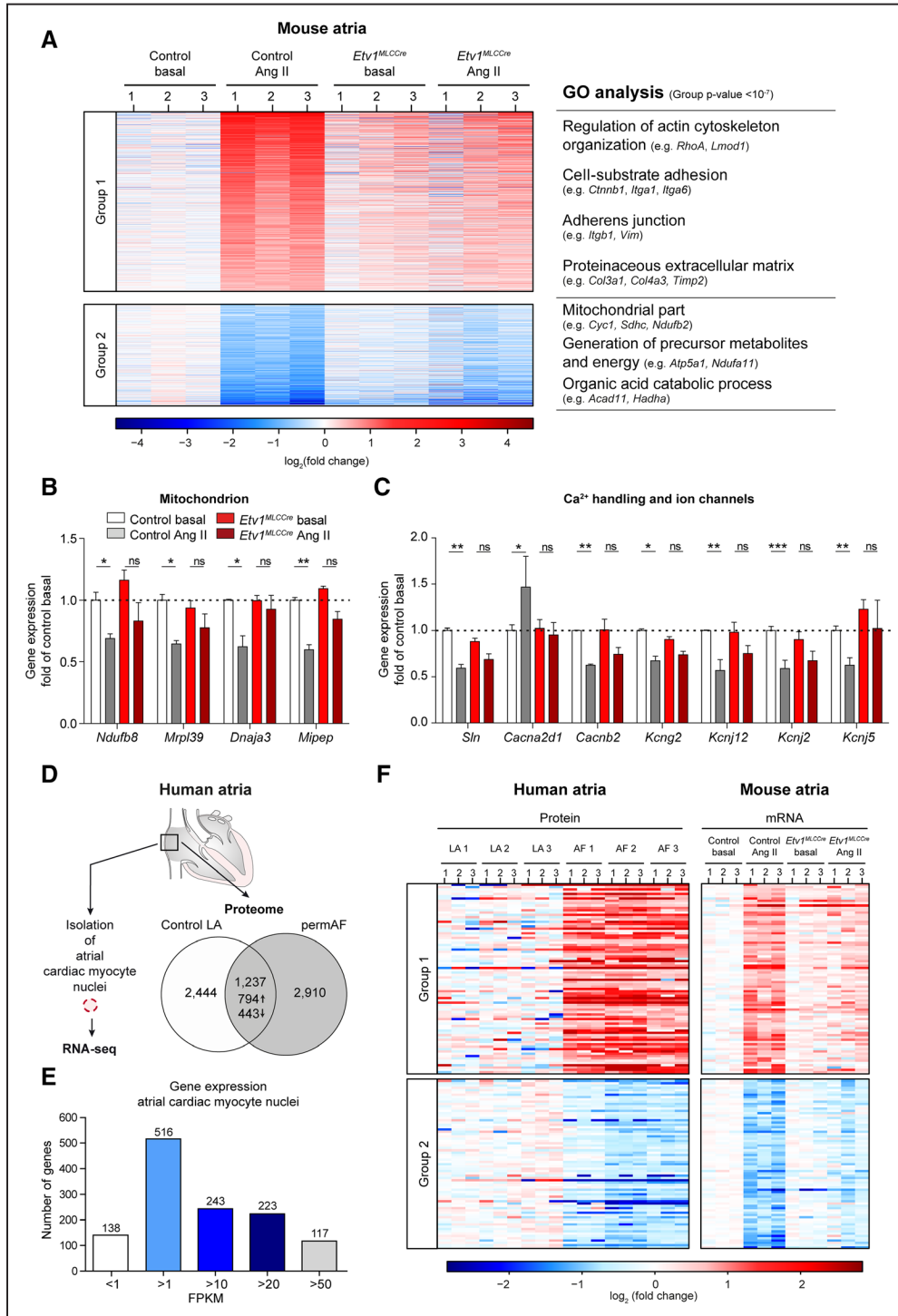


**Figure 5. Ablation of ETV1 (E twenty-six variant 1) prevents Ang (angiotensin) II-induced atrial gene expression changes.** **A**, Heat map of gene expression analyzed by RNA-seq in left atria from *Etv1<sup>MLCCre</sup>* mice and control mice without and after Ang II stimulation for 2 weeks (n=3 per genotype). Gene ontology (GO) analysis of genes significantly up- (group 1) or downregulated (group 2) by Ang II stimulation in control atria without significant changes in *Etv1<sup>MLCCre</sup>* atria (ClueGO). **B**, **C**, Gene expression of mitochondrial-associated genes (**B**), genes involved in Ca<sup>2+</sup> handling and ion channel-coding genes (**C**) in control and *Etv1<sup>MLCCre</sup>* atria without and after Ang II stimulation analyzed by RNA-seq (n=3 per genotype). **D**, Scheme of the experimental procedure for generation of human atrial proteome and isolation of atrial cardiac myocyte nuclei. Venn diagram showing differentially expressed proteins in atria from patients with permanent atrial fibrillation (AF) compared with control left atria (LA). **E**, Gene expression of overlapping proteins/genes in human atrial cardiac myocyte nuclei (FPKM: fragments per kilobase per million mapped reads). **F**, Heat map showing differentially expressed proteins in 3 AF patients (AF 1–3) compared with 3 healthy human left atria (LA 1–3; ANOVA, FDR (false discovery rate; <0.05) overlapping with gene expression changes in left atria from *Etv1<sup>MLCCre</sup>* and control mice without and after Ang II stimulation for 2 weeks (n=3 per genotype). Mean±SEM; \*q<0.05; \*\*q<0.01; \*\*\*q<0.001. ns indicates not significant.

all cell types throughout development and postnatal life. This is in contrast with our mouse model, which relies on Cre-mediated ablation of *Etv1* expression in cardiac myocytes

under control of the myosin light chain (*My17*, *MLC2a-Cre*) promoter starting at embryonic day E7.5.<sup>15</sup> Constitutive ETV1 ablation<sup>34</sup> led to lengthening of the P wave, PR interval, QRS

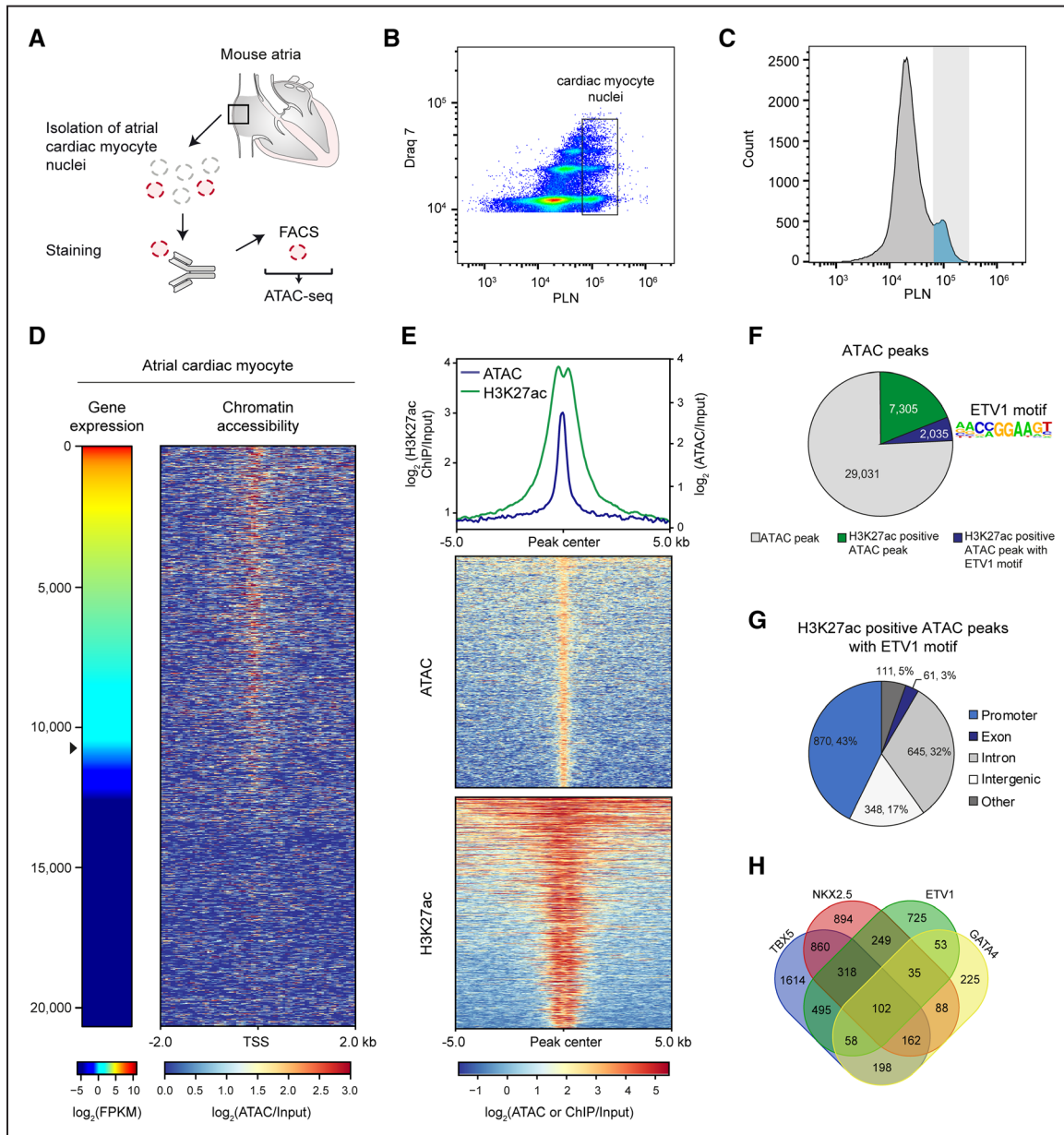


**Figure 6. Chromatin accessibility and gene expression in mouse atrial cardiac myocytes.** **A**, Isolation of atrial cardiac myocyte nuclei from wild-type mouse atrial tissue via fluorescence-assisted cell sorting (FACS). **B**, Fluorescence-assisted sorting of mouse atrial cardiac myocyte nuclei. Draq7<sup>pos</sup> and phospholamban-positive (PLN<sup>pos</sup>) atrial cardiac myocyte nuclei are shown in the box. **C**, Representative histogram of sorted nuclei. **D**, Heat maps of atrial cardiac myocyte gene expression and chromatin accessibility (ATAC). Genes were ranked according to mean expression levels measured by RNA-seq (n=6). Arrow head indicates 1 FPKM (fragments per kilobase per million mapped reads) gene expression level. **E**, Chromatin accessibility and corresponding histone modification H3K27ac profiles. **F**, Pie chart illustrating the number of assay for transposase-accessible chromatin (ATAC) peaks (>2-fold,  $q < 0.05$ ) overlapping with H3K27ac peaks (green and blue) and containing ETV1 (E twenty-six variant 1) motifs (blue). **G**, Pie chart showing the genomic distribution of H3K27ac positive ATAC peaks with ETV1 motif. **H**, Venn diagram of H3K27ac positive ATAC peaks with ETV1, TBX5, NKX2.5 (NK2 homeobox 5), and GATA4 (GATA-binding protein-4) transcription factor motifs. TSS indicates transcription start site.

interval, and to bundle branch block in 30% of the KO mice at postnatal day P18.<sup>34</sup> In contrast, cardiac myocyte-specific loss of ETV1 did not cause any obvious conduction deficits in adult mice (Online Figure VIII), suggesting that ablation of ETV1 by the MLC2a-Cre led to a more subtle phenotype when compared with the constitutive ablation. In addition, in fetal stages of mouse heart development, *MLC2a* expression is confined to the atrial working myocardium, the AV node, but it was undetectable in the bundle of His and the ventricular conduction system.<sup>35</sup> Thus, regional expression of

MLC2a-Cre during heart development in the present model may contribute to the specific phenotype. However, similar to our model, general loss of ETV1 did not affect ventricular structure and function.<sup>34</sup>

ETV1 is a nuclear target of several intracellular signaling cascades. It was shown that ETV1 is activated by the Ras-MAPK pathway.<sup>36</sup> In addition, other kinases downstream of the ERK (extracellular signal-regulated kinase),<sup>36</sup> like the MSK1 (mitogen- and stress-activated protein kinase 1)<sup>37</sup> or the 90-kDa RSK1 (ribosomal S6 kinase 1),<sup>38</sup> phosphorylate, and

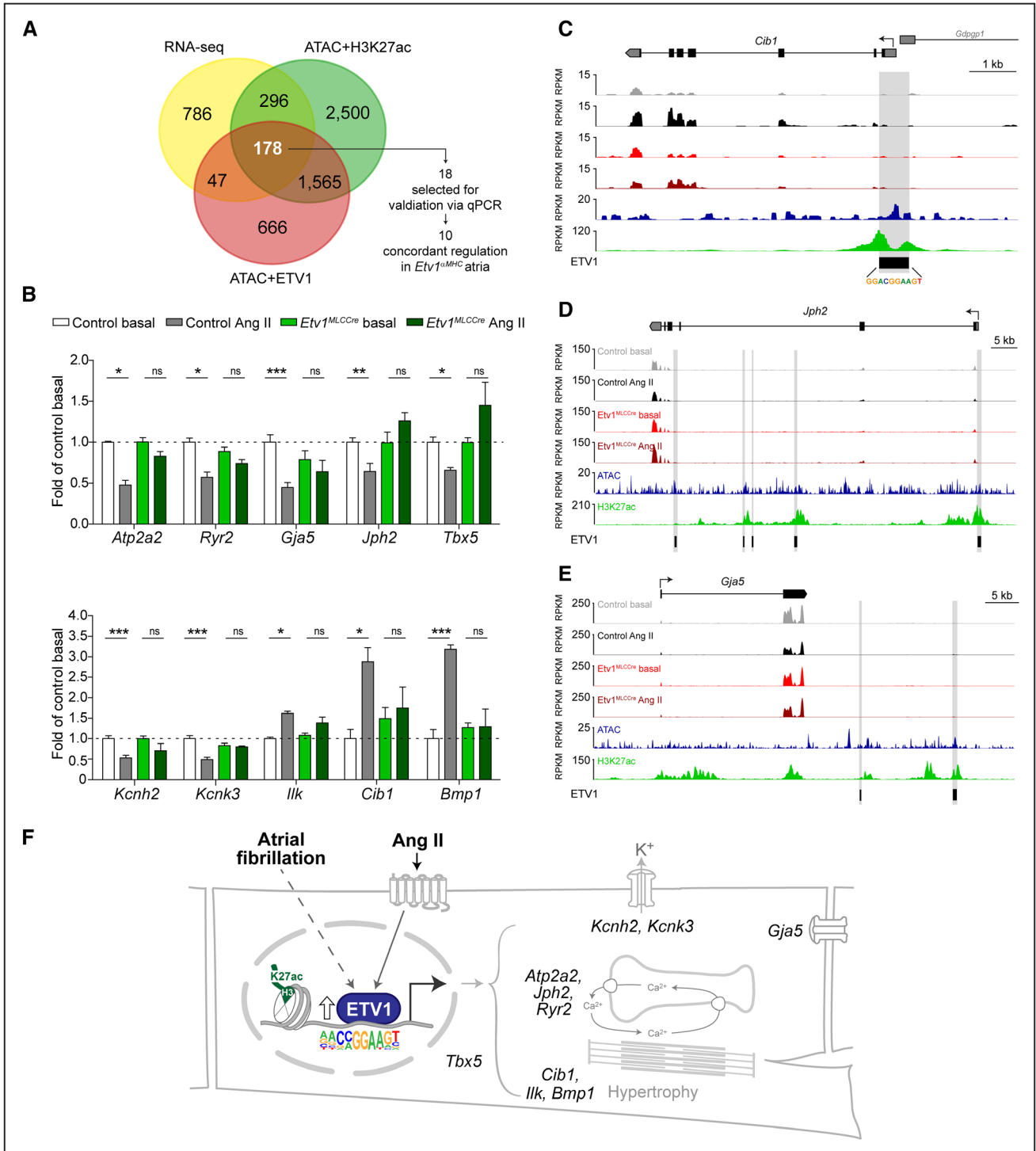


**Figure 7. Identification of ETV1 (E twenty-six variant 1) target genes in atrial cardiac myocytes.** **A**, Venn diagram showing the overlap of Ang (angiotensin) II/ETV1-dependent gene expression changes (RNA-seq), active accessible regions (assay for transposase-accessible chromatin [ATAC]+H3K27ac) and accessible regions including ETV1-binding motifs (ATAC+ETV1). Eighteen out of 178 genes were selected for validation via RT-qPCR. **B**, Gene expression analyzed by RNA-seq in left atria from *Etv1*<sup>MLCCre</sup> mice and respective control mice without and after Ang II stimulation for 2 weeks (n=3 per genotype). **C–E**, Original traces of genetic loci containing calcium and integrin binding 1 (*Cib1*) (**C**), junctophilin 2 (*Jph2*) (**D**), and gap junction protein  $\alpha$  5 (*Gja5*) (**E**). Traces include mRNA expression in atria from control and *Etv1*<sup>MLCCre</sup> mice without and after 2 weeks of Ang II stimulation, ATAC (blue) and H3K27ac histone modification (green) in atrial cardiac myocytes. Active accessible regions containing ETV1 motifs are highlighted in gray. **F**, Overview summarizing ETV1 upregulation and ETV1 target genes in atrial cardiac myocytes. Mean $\pm$ SEM; \* $q$ <0.05; \*\* $q$ <0.01; \*\*\* $q$ <0.001.

active ETV1 and its cofactors. Thus, ETV1 can be activated by signaling pathways initiated by GPCR that activate  $G_s$  or  $G_{q/11}$  heterotrimeric G proteins, respectively.

The GPCR agonist Ang II plays an important role in atrial remodeling and fibrosis.<sup>29</sup> To evaluate the ETV1-dependent effects on atrial remodeling, we treated ETV1-deficient mice

and control mice with Ang II for 2 weeks. We found that ETV1-deficient mice were protected from Ang II-mediated atrial remodeling, whereas control animals showed a clear induction of atrial fibrosis. Previous work has shown that angiotensin-converting enzyme and ERK1/2 expression were increased in patients with AF.<sup>39</sup> Furthermore, mice with cardiac  $G\alpha_q$  overexpression develop spontaneous AF, atrial fibrosis, and dilatation.<sup>40</sup> These results suggest that ETV1 operates as a transcriptional target downstream of Ang II-induced activation of MAPKs in atrial remodeling.

The pathophysiology of AF is complex and includes features like electrical remodeling, structural remodeling, autonomic nervous system changes,  $Ca^{2+}$  handling abnormalities, and a wide spectrum of molecular changes.<sup>2</sup> To identify the molecular mechanism underlying the ETV1-dependent protection from Ang II-induced atrial remodeling, we identified active *cis*-regulatory elements in mouse atrial cardiac myocytes using chromatin accessibility (ATAC-seq) and histone status (H3K27ac).

We found—among other genes—an upregulation of the calcium- and integrin-binding protein-1 (*Cib1*) gene in control atria stimulated with Ang II, although *Cib1* was not regulated in ETV1-deficient atria. CIB1-deficient mice showed reduced cardiac hypertrophy, fibrosis, and cardiac dysfunction after pressure overload, whereas cardiac-specific overexpression of CIB1 augmented cardiac hypertrophy after pressure overload or calcineurin signaling.<sup>41</sup> Moreover, CIB1 mRNA and protein expression was upregulated in atrial tissue from patients with AF.<sup>42</sup> The integrin-linked kinase (*Ilk*) is upregulated in cardiac hypertrophy and mice expressing a constitutively active ILK exhibited hypertrophic remodeling.<sup>43</sup> Interestingly, kinase-inactive ILK inhibited the prohypertrophic effect of Ang II on cardiac myocytes.<sup>43</sup> Thus, Ang II-mediated ETV1-dependent upregulation of *Cib1* and *Ilk* may contribute to hypertrophic remodeling of cardiac myocytes.

Besides the structural changes, electrical remodeling has been implicated in human AF.<sup>2</sup> It has been shown that patients with mutations in the  $\alpha$ -subunit of the voltage-gated potassium channel, encoded by the *KCNH2* gene, present with higher incidence of AF.<sup>44</sup> Our results reveal Ang II-mediated downregulation of *Kcnh2*, whereas ETV1 ablation prevented this downregulation. KCNH2 is responsible for the rapidly repolarizing potassium current (*IKr*) in atrial and ventricular cardiac myocytes<sup>44</sup> and may contribute to action potential duration changes in AF.

Not only changes in ion channel expression but also gap junction remodeling, inducing impaired cell-cell coupling, contributes to conduction abnormalities.<sup>45</sup> The cardiac gap junction protein  $\alpha 5$  (*Gja5*, connexin 40) was downregulated after Ang II stimulation in control atria but showed no regulation in ETV1-deficient atria. *GJA5* is selectively expressed in atrial cardiac myocytes,<sup>46</sup> and *GJA5*-deficient mice showed predispositions to arrhythmias.<sup>47</sup> Moreover, human *GJA5* gene variants were shown to be associated with AF.<sup>48</sup>

Neither loss nor overexpression of *Etv1* elicited a primary ventricular phenotype. Differential chromatin accessibility between atrial and ventricular cardiac myocytes may be one important factor explaining the atrial specificity of the *Etv1* phenotype. Atrial enriched transcription factors like TBX5 may also contribute to this phenotype. In mouse atria, *Tbx5* expression was repressed by Ang II in an ETV1-dependent manner.

Interestingly, *TBX5* mutations have been implicated in AF in human Genome-Wide Association Studies and loss of *Tbx5* in adult mice caused atrial arrhythmia.<sup>30</sup> Many *Tbx5*-dependent genes were also regulated by ETV1 in our study, including *Gja5*, *Ryr2*, *Atp2a2*, and *Kcnh2*.<sup>30,49</sup> Interestingly, almost half of all open chromatin regions in atrial cardiac myocytes containing an ETV1-binding motif also showed TBX5-binding sites. Previously, a direct interaction of ETV1 with the T-box containing factor TPIT (T-box 19) has been demonstrated.<sup>50</sup> Thus, cooperation between ETV1 and cardiac transcription factors may be important to shape the atrial cardiac myocyte transcriptome as it has been identified for other transcription factor pairs.<sup>51</sup>

Several lines of evidence suggest that ETV1 may not only play a role in atrial remodeling in the mouse but also in human AF. First, ETV1 was upregulated in atrial biopsies from patients with permanent AF. Second, the ETV1-dependent transcriptome in mouse atria showed significant overlap with the human atrial proteome of patients with permanent AF. Third, a recent genome-wide association study showed a strong association of an *ETV1* SNP (single nucleotide polymorphism) with atrial conduction defects.<sup>34</sup> Taken together, our results strongly support that ETV1 orchestrates a transcriptional network that drives atrial remodeling.

## Acknowledgments

We thank Claudia Domisch and Birgit Scherer (University of Freiburg, Germany) for technical assistance. We acknowledge the support of the Freiburg Galaxy Team, Rolf Backofen and Björn Grüning (University of Freiburg, Germany), Larissa Fabritz (University of Birmingham, United Kingdom) for advice on ECG analysis, and Ali El-Armouche (Technische Universität Dresden) for atrial tissue samples.

## Sources of Funding

This study was supported by the Deutsche Forschungsgemeinschaft (SFB992 project B03, DFG HE 2073/5-1), the BIOS Centre for Biological Signalling Studies, and PharmCompNet.

## Disclosures

None.

## References

- Kirchhof P, Benussi S, Kotecha D, et al. 2016 ESC Guidelines for the management of atrial fibrillation developed in collaboration with EACTS. *Rev Esp Cardiol (Engl Ed)*. 2017;70:50.
- Nattel S, Harada M. Atrial remodeling and atrial fibrillation: recent advances and translational perspectives. *J Am Coll Cardiol*. 2014;63:2335–2345. doi: 10.1016/j.jacc.2014.02.555.
- Heijman J, Voigt N, Nattel S, Dobrev D. Cellular and molecular electrophysiology of atrial fibrillation initiation, maintenance, and progression. *Circ Res*. 2014;114:1483–1499. doi: 10.1161/CIRCRESAHA.114.302226.
- Lin CS, Pan CH. Regulatory mechanisms of atrial fibrotic remodeling in atrial fibrillation. *Cell Mol Life Sci*. 2008;65:1489–1508. doi: 10.1007/s00018-008-7408-8.
- Paul M, Poyan Mehr A, Kreutz R. Physiology of local renin-angiotensin systems. *Physiol Rev*. 2006;86:747–803. doi: 10.1152/physrev.00036.2005.
- Tamargo J, López-Sendón J. Novel therapeutic targets for the treatment of heart failure. *Nat Rev Drug Discov*. 2011;10:536–555. doi: 10.1038/nrd3431.
- Hein L, Stevens ME, Barsh GS, Pratt RE, Kobilka BK, Dzau VJ. Overexpression of angiotensin AT1 receptor transgene in the mouse myocardium produces a lethal phenotype associated with myocyte hyperplasia and heart block. *Proc Natl Acad Sci USA*. 1997;94:6391–6396.
- Xiao HD, Fuchs S, Frenzel K, Teng L, Bernstein KE. Circulating versus local angiotensin II in blood pressure control: lessons from tissue-specific expression of angiotensin-converting enzyme (ACE). *Crit Rev Eukaryot Gene Expr*. 2004;14:137–145.

9. Heineke J, Molkenin JD. Regulation of cardiac hypertrophy by intracellular signalling pathways. *Nat Rev Mol Cell Biol.* 2006;7:589–600. doi: 10.1038/nrm1983.
10. Schmid E, Neef S, Berlin C, et al. Cardiac RKIP induces a beneficial  $\beta$ -adrenoceptor-dependent positive inotropy. *Nat Med.* 2015;21:1298–1306. doi: 10.1038/nm.3972.
11. van Berlo JH, Mailliet M, Molkenin JD. Signaling effectors underlying pathologic growth and remodeling of the heart. *J Clin Invest.* 2013;123:37–45. doi: 10.1172/JCI62839.
12. Akazawa H, Komuro I. Roles of cardiac transcription factors in cardiac hypertrophy. *Circ Res.* 2003;92:1079–1088. doi: 10.1161/01.RES.0000072977.86706.23.
13. Mahida S. Transcription factors and atrial fibrillation. *Cardiovasc Res.* 2014;101:194–202. doi: 10.1093/cvr/cvt261.
14. Patel TD, Kramer I, Kucera J, Niederkofler V, Jessell TM, Arber S, Snider WD. Peripheral NT3 signaling is required for ETS protein expression and central patterning of proprioceptive sensory afferents. *Neuron.* 2003;38:403–416.
15. Wettschurek N, Rütten H, Zywiets A, Gehring D, Wilkie TM, Chen J, Chien KR, Offermanns S. Absence of pressure overload induced myocardial hypertrophy after conditional inactivation of Galpha1 in cardiomyocytes. *Nat Med.* 2001;7:1236–1240. doi: 10.1038/nm1101-1236.
16. Mayer SC, Gilsbach R, Preissl S, et al. Adrenergic repression of the epigenetic reader MeCP2 facilitates cardiac adaptation in chronic heart failure. *Circ Res.* 2015;117:622–633. doi: 10.1161/CIRCRESAHA.115.306721.
17. Preissl S, Schwaderer M, Raulf A, Hesse M, Grüning BA, Köbele C, Backofen R, Fleischmann BK, Hein L, Gilsbach R. Deciphering the epigenetic code of cardiac myocyte transcription. *Circ Res.* 2015;117:413–423. doi: 10.1161/CIRCRESAHA.115.306337.
18. Buenrostro JD, Wu B, Chang HY, Greenleaf WJ. ATAC-seq: a method for assaying chromatin accessibility genome-wide. *Curr Protoc Mol Biol.* 2015;109:21.29.1–21.29.9. doi: 10.1002/0471142727.mb2129s109.
19. Claycomb WC, Lanson NA Jr, Stallworth BS, Egeland DB, Delcarpio JB, Bahinski A, Izzo NJ Jr. HL-1 cells: a cardiac muscle cell line that contracts and retains phenotypic characteristics of the adult cardiomyocyte. *Proc Natl Acad Sci USA.* 1998;95:2979–2984.
20. Afgan E, Baker D, van den Beek M, et al. The Galaxy platform for accessible, reproducible and collaborative biomedical analyses: 2016 update. *Nucleic Acids Res.* 2016;44:W3–W10. doi: 10.1093/nar/gkw343.
21. Langmead B, Trapnell C, Pop M, Salzberg SL. Ultrafast and memory-efficient alignment of short DNA sequences to the human genome. *Genome Biol.* 2009;10:R25. doi: 10.1186/gb-2009-10-3-r25.
22. Dobin A, Davis CA, Schlesinger F, Drenkow J, Zaleski C, Jha S, Batut P, Chaisson M, Gingeras TR. STAR: ultrafast universal RNA-seq aligner. *Bioinformatics.* 2013;29:15–21. doi: 10.1093/bioinformatics/bts635.
23. Trapnell C, Williams BA, Pertea G, Mortazavi A, Kwan G, van Baren MJ, Salzberg SL, Wold BJ, Pachter L. Transcript assembly and quantification by RNA-Seq reveals unannotated transcripts and isoform switching during cell differentiation. *Nat Biotechnol.* 2010;28:511–515. doi: 10.1038/nbt.1621.
24. Ramírez F, Ryan DP, Grüning B, Bhardwaj V, Kilpert F, Richter AS, Heyne S, Dündar F, Manke T, deepTools2: a next generation web server for deep-sequencing data analysis. *Nucleic Acids Res.* 2016;44:W160–W165. doi: 10.1093/nar/gkw257.
25. Zhang Y, Liu T, Meyer CA, Eeckhoutte J, Johnson DS, Bernstein BE, Nusbaum C, Myers RM, Brown M, Li W, Liu XS. Model-based analysis of ChIP-Seq (MACS). *Genome Biol.* 2008;9:R137. doi: 10.1186/gb-2008-9-9-r137.
26. Doll S, Dreßen M, Geyer PE, Itzhak DN, Braun C, Doppler SA, Meier F, Deutsch MA, Lahm H, Lange R, Krane M, Mann M. Region and cell-type resolved quantitative proteomic map of the human heart. *Nat Commun.* 2017;8:1469. doi: 10.1038/s41467-017-01747-2.
27. Vedantham V, Galang G, Evangelista M, Deo RC, Srivastava D. RNA sequencing of mouse sinoatrial node reveals an upstream regulatory role for Islet-1 in cardiac pacemaker cells. *Circ Res.* 2015;116:797–803. doi: 10.1161/CIRCRESAHA.116.305913.
28. Esperer HD, Esperer C, Cohen RJ. Cardiac arrhythmias imprint specific signatures on Lorenz plots. *Ann Noninvasive Electrocardiol.* 2008;13:44–60. doi: 10.1111/j.1542-474X.2007.00200.x.
29. Burstein B, Nattel S. Atrial fibrosis: mechanisms and clinical relevance in atrial fibrillation. *J Am Coll Cardiol.* 2008;51:802–809. doi: 10.1016/j.jacc.2007.09.064.
30. Nadadur RD, Broman MT, Boukens B, et al. Pitx2 modulates a Tbx5-dependent gene regulatory network to maintain atrial rhythm. *Sci Transl Med.* 2016;8:354ra115. doi: 10.1126/scitranslmed.aaf4891.
31. Gutierrez-Roelens I, De Roy L, Ovaert C, Sluysmans T, Devriendt K, Brunner HG, Vikkula M. A novel CSX/NKX2-5 mutation causes autosomal-dominant AV block: are atrial fibrillation and syncope part of the phenotype? *Eur J Hum Genet.* 2006;14:1313–1316. doi: 10.1038/sj.ejhg.5201702.
32. Yang YQ, Wang MY, Zhang XL, Tan HW, Shi HF, Jiang WF, Wang XH, Fang WY, Liu X. GATA4 loss-of-function mutations in familial atrial fibrillation. *Clin Chim Acta.* 2011;412:1825–1830. doi: 10.1016/j.cca.2011.06.017.
33. Yang YQ, Li L, Wang J, Liu XY, Chen XZ, Zhang W, Wang XZ, Jiang JQ, Liu X, Fang WY. A novel GATA4 loss-of-function mutation associated with congenital ventricular septal defect. *Pediatr Cardiol.* 2012;33:539–546. doi: 10.1007/s00246-011-0146-y.
34. Shekhar A, Lin X, Liu FY, Zhang J, Mo H, Bastarache L, Denny JC, Cox NJ, Delmar M, Roden DM, Fishman GI, Park DS. Transcription factor ETV1 is essential for rapid conduction in the heart. *J Clin Invest.* 2016;126:4444–4459. doi: 10.1172/JCI87968.
35. Franco D, Icardo JM. Molecular characterization of the ventricular conduction system in the developing mouse heart: topographical correlation in normal and congenitally malformed hearts. *Cardiovasc Res.* 2001;49:417–429.
36. Janknecht R. Analysis of the ERK-stimulated ETS transcription factor ER81. *Mol Cell Biol.* 1996;16:1550–1556.
37. Janknecht R. Regulation of the ER81 transcription factor and its coactivators by mitogen- and stress-activated protein kinase 1 (MSK1). *Oncogene.* 2003;22:746–755. doi: 10.1038/sj.onc.1206185.
38. Wu J, Janknecht R. Regulation of the ETS transcription factor ER81 by the 90-kDa ribosomal S6 kinase 1 and protein kinase A. *J Biol Chem.* 2002;277:42669–42679. doi: 10.1074/jbc.M205510200.
39. Goette A, Staack T, Röcken C, Arndt M, Geller JC, Huth C, Ansoerge S, Klein HU, Lendeckel U. Increased expression of extracellular signal-regulated kinase and angiotensin-converting enzyme in human atria during atrial fibrillation. *J Am Coll Cardiol.* 2000;35:1669–1677.
40. Hirose M, Takeishi Y, Niizeki T, Shimajo H, Nakada T, Kubota I, Nakayama J, Mende U, Yamada M. Diacylglycerol kinase zeta inhibits G(alpha)q-induced atrial remodeling in transgenic mice. *Heart Rhythm.* 2009;6:78–84. doi: 10.1016/j.hrthm.2008.10.018.
41. Heineke J, Auger-Messier M, Correll RN, Xu J, Benard MJ, Yuan W, Drexler H, Parise LV, Molkenin JD. CIB1 is a regulator of pathological cardiac hypertrophy. *Nat Med.* 2010;16:872–879. doi: 10.1038/nm.2181.
42. Zhao F, Zhang S, Chen L, Wu Y, Qin J, Shao Y, Wang X, Chen Y. Calcium- and integrin-binding protein-1 and calcineurin are upregulated in the right atrial myocardium of patients with atrial fibrillation. *Europace.* 2012;14:1726–1733. doi: 10.1093/europace/eus149.
43. Lu H, Fedak PW, Dai X, Du C, Zhou YQ, Henkelman M, Mongroo PS, Lau A, Yamabi H, Hinek A, Husain M, Hannigan G, Coles JG. Integrin-linked kinase expression is elevated in human cardiac hypertrophy and induces hypertrophy in transgenic mice. *Circulation.* 2006;114:2271–2279. doi: 10.1161/CIRCULATIONAHA.106.642330.
44. Sinner MF, Pfeufer A, Akyol M, et al. The non-synonymous coding IKr-channel variant KCNH2-K897T is associated with atrial fibrillation: results from a systematic candidate gene-based analysis of KCNH2 (HERG). *Eur Heart J.* 2008;29:907–914. doi: 10.1093/eurheartj/ehm619.
45. Lo CW. Role of gap junctions in cardiac conduction and development: insights from the connexin knockout mice. *Circ Res.* 2000;87:346–348.
46. Gollob MH, Jones DL, Krahn AD, et al. Somatic mutations in the connexin 40 gene (GJA5) in atrial fibrillation. *N Engl J Med.* 2006;354:2677–2688. doi: 10.1056/NEJMoa052800.
47. Kirchhoff S, Nelles E, Hagedorff A, Krüger O, Traub O, Willecke K. Reduced cardiac conduction velocity and predisposition to arrhythmias in connexin40-deficient mice. *Curr Biol.* 1998;8:299–302.
48. Wirka RC, Gore S, Van Wagoner DR, Arking DE, Lubitz SA, Lunetta KL, Benjamin EJ, Alonso A, Ellinor PT, Barnard J, Chung MK, Smith JD. A common connexin-40 gene promoter variant affects connexin-40 expression in human atria and is associated with atrial fibrillation. *Circ Arrhythm Electrophysiol.* 2011;4:87–93. doi: 10.1161/CIRCEP.110.959726.
49. Yang XH, Nadadur RD, Hilvering CR, et al. Transcription-factor-dependent enhancer transcription defines a gene regulatory network for cardiac rhythm. *Elife.* 2017;6:e31683.
50. Budry L, Couture C, Balsalobre A, Drouin J. The Ets factor ETV1 interacts with Tpit protein for pituitary pro-opiomelanocortin (POMC) gene transcription. *J Biol Chem.* 2011;286:25387–25396. doi: 10.1074/jbc.M110.202788.
51. Luna-Zurita L, Stirmimann CU, Glatt S, Kaynak BL, Thomas S, Baudin F, Samee MA, He D, Small EM, Mileikovskiy M, Nagy A, Holloway AK, Pollard KS, Müller CW, Bruneau BG. Complex interdependence regulates heterotypic transcription factor distribution and coordinates cardiogenesis. *Cell.* 2016;164:999–1014. doi: 10.1016/j.cell.2016.01.004.